Internal Conversion in 1-Aminonaphthalenes. Influence of Amino Twist Angle

Ingo Rückert, Attila Demeter,† Olaf Morawski, Wolfgang Kühnle, Erich Tauer, and Klaas A. Zachariasse*

Max-Planck-Institut für biophysikalische Chemie-Spektroskopie und Photochemische Kinetik-D-37070 Göttingen, Germany

Received: October 21, 1998; In Final Form: January 28, 1999

With the 1-aminonaphthalenes 1N5 and 1DMAN a fast radiationless process occurs in *n*-hexane, diethyl ether, and acetonitrile, which is shown to be internal conversion (IC). The IC reaction is slower with 1N4 and much less efficient with 1MAN and 1AN. This IC process is thermally activated and slows down with increasing solvent polarity, due to a larger IC activation energy. In the ground state S_0, the amino twist angle θ relative to the naphthalene plane increases in the order 1MAN, 1AN, 1N4, 1N5, 1DMAN, as derived from absorption and fluorescence spectra, ^{1}H NMR spectra, ground-state dipole moments, and ab initio calculations. For the five 1-aminonaphthalenes in the equilibrated S_1 state, the twist angle and the radiative rate constant have similar values. The different IC efficiences of these molecules are therefore determined by the structural differences (amino twist angle) between S_1 and S_0. A correlation is found between the IC efficiency in these molecules and the twist angle θ. The IC process to S_0 starts from the equilibrated S_1 state, which is vibronically coupled with S_2 due to a small energy gap $\Delta E(S_1,S_2)$. It is therefore concluded that the extent of vibronic coupling and the magnitude of the twist angle θ are the determining factors in the IC process.

Introduction

The replacement of the amino substituent in 4-(dimethylamino)benzonitrile (DMABN) by a pyrrolidinyl or an azetidinyl group, giving either 4-(*N*-azetidinyl)benzonitrile (P4C) or 4-(*N*-pyrrolidinyl)benzonitrile (P5C), leads to a considerable decrease in the intramolecular charge transfer (ICT) efficiency, especially in the case of P4C.[1−5] The difference between P4C and P5C comes from a substantially larger ICT activation energy for the former molecule, determined by the amino nitrogen inversion barrier.[3,5]

A similar phenomenon has been observed for the ICT reaction in 1-amino-4-cyanonaphthalenes. With 1-(*N*-azetidinyl)-4-cyanonaphthalene (1N4C), a dual fluorescence from a charge transfer (CT) state next to that from the initially prepared locally excited (LE) state has not been observed,[6] not even in polar solvents such as acetonitrile, in contrast to the dual CT and LE emission found with 1-(dimethylamino)-4-cyanonaphthalene (1DMACN).[4−7]

These differences in photophysical behavior clearly show that the presence of a pyrrolidinyl and especially an azetidinyl group can lead to a reduction in the ICT efficiency as compared with the dimethylamino derivatives. In the present paper the influence of replacing the dimethylamino group of 1-(dimethylamino)-naphthalene (1DMAN) by a heterocyclic azetidinyl or pyrrolidinyl group, resulting in 1-(*N*-azetidinyl)naphthalene (1N4) or 1-(*N*-pyrrolidinyl)naphthalene (1N5), on the photophysical behavior of these compounds will be discussed.

With 1DMAN, a thermally activated internal conversion (IC) takes place, which reduces the fluorescence decay time τ as well as the quantum yield Φ_f.[8−11] This IC process is especially efficient in nonpolar solvents such as *n*-alkanes at ambient temperature.[10] As an example, for 1DMAN in *n*-hexane at 25 °C, a decay time τ of 120 ps and a quantum yield Φ_f of 0.01 has been determined.[10] These data should be compared with the values of 6.65 or 7.80 ns for τ and 0.44 or 0.58 for Φ_f of 1-aminonaphthalene (1AN) or 1-(methylamino)naphthalene (1MAN), respectively, under these conditions, for which molecules only a weak IC reaction occurs.[10] From the fact that the dimethylamino group in 1DMAN is twisted out of the naphthalene plane in the electronic ground state, whereas the molecule becomes more planar in the equilibrated S_1 state,[10,11] it follows that the amino substituent undergoes an antitwist movement toward planarity with the naphthalene moiety during the relaxation process.

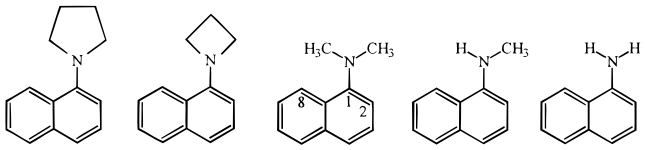

The efficiency of the IC reaction with 1DMAN decreases with increasing solvent polarity.[9−11] This decrease is caused mainly by an increase in the IC activation energy E_{IC}.[10] The occurrence of the IC phenomenon and its polarity dependence have been attributed to vibronic coupling between the two lowest singlet excited states S_1 and S_2, the energy gap $\Delta E(S_1,S_2)$ becoming larger when the solvent polarity increases.[10] It has been suggested that, as far as the vibronic coupling is concerned, the IC process in 1DMAN is photophysically analogous to the ICT reaction in DMABN.[10]

Experimental Section

1N4 was synthesized by reacting 1-fluoronaphthalene (Aldrich) with azetidine (Merck), following the procedure used for

* Author to whom correspondence should be addressed. Fax: +49 551 201 1501. E-mail: kzachar@gwdg.de.

† On leave from the Institute of Chemistry, Chemical Research Center, Hungarian Academy of Sciences, P.O. Box 17, 1525 Budapest, Hungary.

10.1021/jp984115p CCC: $18.00
Published on Web 03/11/1999

P4C.[13] 1N5 was made from naphthalene-1-yl-(4-phenoxybutyl)-amine and $AlCl_3$.[14] This amine resulted from a reaction between 1AN (Merck) and 4-methoxybutylbromide.[15] A synthesis procedure similar to that employed to obtain 1N4 did not lead to the desired product. 1DMAN was obtained from Fluka. 1MAN was made by reacting 1AN with formic acid.[16] With all these molecules HPLC was the last purification step.

The solvent *n*-hexane (Merck) was used as received. Diethyl ether (Merck−Uvasol) and acetonitrile (Baker) were chromatographed over Al_2O_3 just prior to use. The solutions, with an optical density between 0.6 and 1.0 for the maximum of the first band in the absorption spectrum, were deaerated by bubbling with nitrogen for 15 min.

The fluorescence spectra were measured with a quantum-corrected Shimadzu RF-5000PC spectrofluorimeter. The fluorescence decay times were determined with picosecond laser or nanosecond flashlamp single-photon counting (SPC) setups. These systems were described previously.[10,17,18] The picosecond SPC equipment consists, in brief, of a mode-locked argon ion laser (Coherent, Innova 100-10) and a synchronized dye−laser system (Coherent 702-1CD, Rhodamine 6G). The outcoupled light is frequency-doubled (298 nm) in a $LiIO_3$ crystal. The fluorescence and scatter (Ludox) records are measured with a Hamamatsu R3809 MCP photomultiplier (−3000 V). Alternatively, a picosecond laser system consisting of a mode-locked titanium−sapphire laser (Coherent, MIRA 900-F) pumped by an argon ion laser (Coherent, Innova 415) was used. By frequency-doubling and sum-frequency generation a wavelength of 300 nm is reached. The instrument response function has a half-width of 25−35 ps. The fluorescence is detected at magic angle (54.7°).

The intersystem crossing yield Φ_{ISC} from the equilibrated S_1 state to the lowest triplet state T_1 was measured by T−T absorption, using a method based on triplet energy transfer with 9,10-dichloroanthracene as the acceptor.[19−21] As a reference substance, either *N*-methyl-1,8-naphthalimide in *n*-hexane or benzophenone in acetonitrile was used. For both substances, Φ_{ISC} was taken to be equal to 1.0.[21−23] The solutions used in these experiments were degassed employing the freeze−pump−thaw method.

Results and Discussion

Fluorescence, Intersystem Crossing, and Internal Conversion. The fluorescence spectra of the 1-aminonaphthalenes 1N5, 1N4, 1DMAN, 1MAN, and 1AN consist of a single emission band (Figure 1). This is the case in *n*-hexane as well as in the more polar solvents diethyl ether[6] and acetonitrile. There is no sign of the dual fluorescence that was previously postulated for 1AN.[24] In contrast to this spectral uniformity, the fluorescence quantum yields of the naphthylamines are strikingly different.

In *n*-hexane at 25 °C, the fluorescence quantum yields Φ_f of 1N5 (0.007), 1N4 (0.14), and 1DMAN (0.010) are considerably smaller than those of 1MAN (0.58) and 1AN (0.44) (Table 1). To determine the cause for the low Φ_f values of the three former molecules, the yields for intersystem crossing (ISC) and internal conversion (IC) were determined.

The intersystem crossing yield Φ_{ISC} was measured by T−T absorption, giving in *n*-hexane at 25 °C relatively small values for 1DMAN (0.02), 1N5 (0.03), and 1N4 (0.13), see Table 1, as compared with those for 1MAN (0.43) and 1AN (0.46). From these data and Φ_f, the internal conversion yield Φ_{IC} can then be calculated by using the expression in eq 1.

$$\phi_{IC} = 1 - \phi_f - \phi_{ISC} \qquad (1)$$

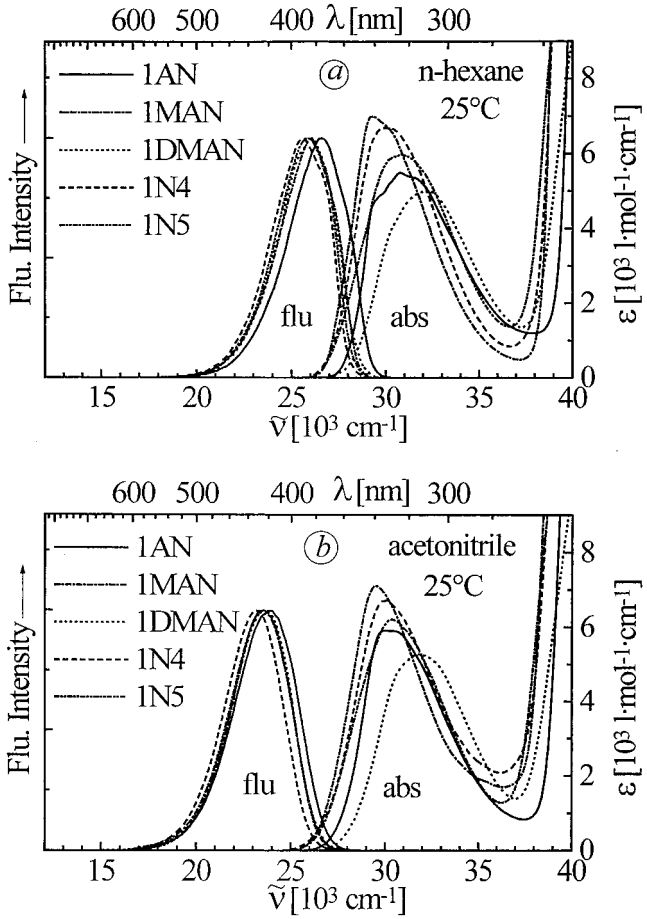

Figure 1. Absorption and normalized fluorescence spectra of 1N5, 1N4, 1DMAN, 1MAN, and 1AN in (a) *n*-hexane and (b) acetonitrile at 25 °C.

It is thereby assumed that no processes other than fluorescence, intersystem crossing, and internal conversion take part in the deactivation of the S_1 state of the 1-naphthylamines, as evidence for the occurrence of photochemical reactions was not found.

It follows from these data, that internal conversion is the major process causing the strong decrease in the fluorescence quantum yield Φ_f and also in the decay time τ (see below) of 1N5 ($\Phi_{IC} = 0.96$) and 1N4 ($\Phi_{IC} = 0.73$) in an unpolar solvent such as *n*-hexane at 25 °C, similar to what has been observed with 1DMAN ($\Phi_{IC} = 0.97$).[10] IC also takes place with 1MAN and 1AN, but with much lower yields of 0.10 and 0.09, respectively (Table 1). In the polar solvent acetonitrile at 25 °C, the yields Φ_{IC} of 1N5, 1N4, and 1DMAN are considerably smaller than in *n*-hexane, see Table 1, especially in the case of 1N4: 0.11 in acetonitrile as compared with 0.73 in *n*-hexane. With 1MAN and 1AN in acetonitrile, appreciable IC does not occur, as the sum of Φ_f and Φ_{ISC} is equal to unity (Table 1).

Temperature Dependence of Fluorescence Quantum Yields. The fluorescence quantum yield Φ_f of the aminonaphthalenes 1N5, 1N4, 1DMAN, and 1AN was determined as a function of temperature in *n*-hexane and acetonitrile (Figure 2). In the case of 1N5, 1DMAN, and 1N4 in *n*-hexane (Figure 2a), Φ_f sharply increases with decreasing temperature. This shows that the fluorescence quenching in these molecules is thermally activated.[10] With 1N4, Φ_f reaches a plateau at ∼−60 °C, whereas such a temperature independence is not observed for the more strongly quenched molecules 1N5 and 1DMAN. For 1DMAN

TABLE 1: Fluorescence Decay Times τ, Yields Φ_i, and Rate Constants k_i of Fluorescence (f), Intersystem Crossing (ISC), and Internal Conversion (IC) and the Arrhenius Parameters k_{IC}^0 and E_{IC} for Internal Conversion (eq 2 and Figure 4)

25 °C	τ [ns]	Φ_f	Φ_{ISC}[a]	Φ_{IC}[b]	k_f [10^7 s^{-1}]	k_{ISC}[c] [10^7 s^{-1}]	k_{IC}[d] [10^7 s^{-1}]	k_{IC}^0[e] [10^{13} s^{-1}]	E_{IC} [kJ mol^{-1}]
					n-Hexane				
1N5	0.082	0.007	0.03	0.96	8.5	40	1200 ± 50	1.1	17 ± 1
1N4	1.73	0.14	0.13	0.73	8.4	8	40 ± 2	1.5	26 ± 1
1DMAN	0.120	0.01	0.02	0.97	8.3	15	830 ± 30	1.2	18 ± 1
1MAN	7.80	0.58	(0.43)[f]	0.04[g]	7.4	4	0.6 ± 0.4	5.8	40 ± 10
1AN	6.65	0.44	0.46	0.09	6.6	7	1.4 ± 0.6	6.4	38 ± 8
					Diethyl Ether				
1N5	0.382	0.031			8.1				
1N4	5.96	0.45			7.6				
1DMAN	0.440	0.032	0.03	0.94	7.3	6	220 ± 10	13	27 ± 2
1MAN	11.7	0.82			7.0				
1AN	12.4	0.78			6.3				
					Acetonitrile				
1N5	4.45	0.24	0.33	0.43	5.3	7	10 ± 2	5.7	33 ± 3
1N4	14.2	0.75	0.14	0.11	5.3	1.0	0.14 ± 0.09	1.4	40 ± 15
1DMAN	4.45	0.21	0.31	0.48	4.6	7	11 ± 2	3.4	31 ± 2
1MAN	17.7	0.92	0.09	0.0	5.2	0.5	[h]		
1AN	18.3	0.86	0.16	0.0	4.7	0.9	[h]		

[a] Determined from T−T absorption. [b] Calculated from $\Phi_{IC} = 1 - \Phi_f - \Phi_{ISC}$, see eq 1. [c] k_{ISC} is calculated from Φ_{ISC}/τ. [d] k_{IC} is obtained by using the Arrhenius expression $k_{IC}^0 \exp(-E_{IC}/RT)$. [e] The uncertainty in the preexponentiel factor k_{IC}^0 is exponentially related with that of the activation energy E_{IC}. [f] Value probably too high due to the exceptional instability of 1MAN. [g] From the temperature dependence of τ (eq 2) a value of 0.38 was obtained for Φ_{ISC}. With the other molecules in the Table, the same values for Φ_{IC} were determined either by T−T absorption or from fitting the τ data (Figure 4). [h] An acceptable fit of the τ data could be achieved without taking k_{IC} into account.

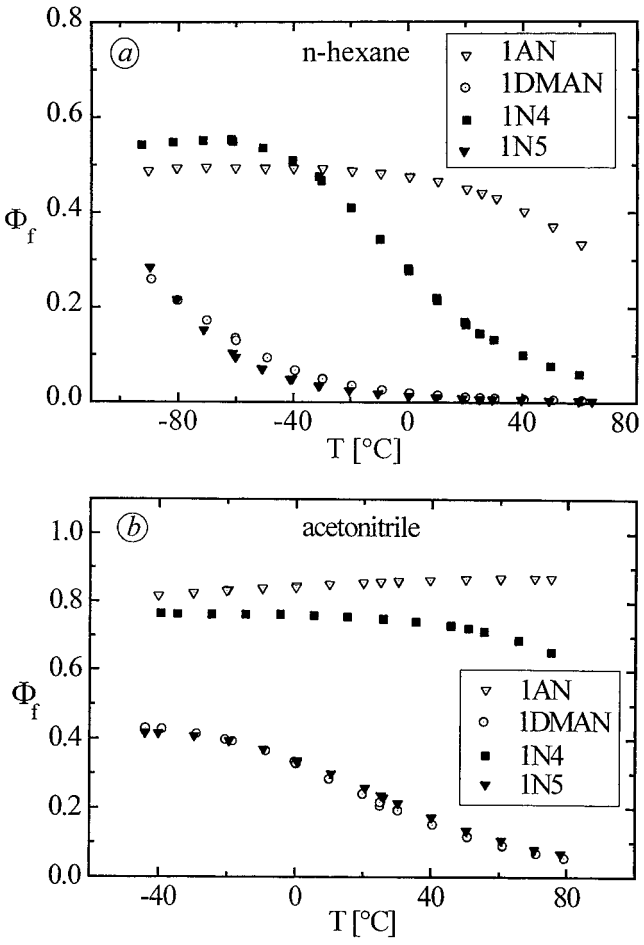

Figure 2. Fluorescence quantum yields Φ_f of 1N5, 1N4, 1DMAN, and 1AN in (a) *n*-hexane and (b) acetonitrile as a function of temperature.

in isopentane, measured down to its melting point (−160 °C), the fluorescence yield only stops to increase upon cooling below −140 °C.[6]

In acetonitrile (Figure 2b), the fluorescence quantum yield of the aminonaphthalenes likewise increases when the temperature is lowered, except for 1AN. The increase of Φ_f for the strongly fluorescent 1AN upon heating, comes from the increase of the predominant radiative rate constant k_f, to be discussed below. The comparison of the Φ_f data for *n*-hexane and acetonitrile in Figure 2 indicates that for 1N5 and 1N4, similar to what has been observed for 1DMAN,[9−11] fluorescence quenching by internal conversion still takes place in acetonitrile, but has become less efficient in this polar solvent.

Fluorescence Decay Times and Radiative Rate Constants at 25 °C. Influence of Solvent Polarity. The fluorescence decays of 1N5, 1N4, 1DMAN, 1MAN, and 1AN in *n*-hexane, diethyl ether, and acetonitrile are single exponential.[6,10,11] The decays of 1N5 and 1N4 in *n*-hexane and acetonitrile at 25 °C are presented in Figure 3. The decay time τ of 1N5 (0.082 ns) in *n*-hexane is much shorter than that of 1MAN (7.80 ns) or 1AN (6.65 ns), with a value even smaller than the 0.120 ns obtained for 1DMAN, see Table 1. Also with 1N4 in *n*-hexane (1.73 ns), a substantial decrease in τ as compared with 1MAN and 1AN is observed (Figure 3c).

The same differences as those found here for τ, appear in the fluorescence quantum yields Φ_f (Table 1), see Figure 2. This means that the radiative rate constant k_f ($= \Phi_f/\tau$) is similar for the five naphthylamines, with a value $\sim 8 \times 10^7$ s^{-1} for 1N5, 1N4, and 1DMAN, and $\sim 7 \times 10^7$ s^{-1} for 1MAN and 1AN (Table 1). From these results it is concluded that the molecular nature of the S_1 state in these compounds does not depend on the structure of the amino substituent.

Upon increasing the solvent polarity (diethyl ether and acetonitrile), the decay times become longer, see Table 1. In acetonitrile at 25 °C, the decay times τ of 1N5 (4.45 ns), 1DMAN (4.45 ns), and 1N4 (14.2 ns) are still shorter than those of 1MAN (17.7 ns) and 1AN (18.3 ns). Again, τ(1N5) and τ(1DMAN) are much smaller than τ(1N4), but k_f and hence the molecular nature of S_1 (see above) does not change. These results show that the excited-state quenching process slows down with increasing solvent polarity,[9−11] but remains more efficient with 1N5 and 1DMAN than in the case of 1N4.

Activation Energies of Internal Conversion from Fluorescence Decay Times. To determine the activation energies E_{IC} of the IC process, the fluorescence decay time τ of the 1-aminonaphthalenes 1N5, 1N4, 1DMAN, 1MAN, and 1AN in *n*-hexane and acetonitrile was measured as a function of temperature, see Figure 4. In contrast to what is observed with 1AN and 1MAN, τ(1N4) in *n*-hexane strongly decreases with increasing temperature, reaching a value of 550 ps at 65 °C (Figure 4a). This decrease is considerably smaller, however, than that obtained with 1N5 in *n*-hexane, for which τ changes from 2.2 ns at −92 °C down to 55 ps at 65 °C (Figure 4a). For 1DMAN a similar temperature dependence is found,[10] see Table 1. In acetonitrile, the temperature dependence of the decay times of 1N5 and 1N4 (Figure 4b) is considerably smaller than that observed in *n*-hexane. Such a behavior has previously also been reported for 1DMAN[10] and was attributed to an increase in the IC activation energy with increasing solvent polarity.

The activation energies E_{IC} were determined by fitting the decay time data in *n*-hexane and acetonitrile as a function of temperature with the expression given in eq 2, where the rate constants k_{IC} and k_{ISC} are given in Arrhenius form and $k_{ISC}(0)$ is the temperature-independent ISC rate constant. In this procedure, a constant value of 5 kJ/mol for the ISC activation energy E_{ISC} is adopted[25] and k_f is taken to be temperature independent. The fits are shown in Figure 4 and the data for k_{IC}^0 and E_{IC} so obtained are listed in Table 1. It is seen that E_{IC} indeed increases with solvent polarity.

$$\frac{1}{\tau} = k_f + k_{IC} + k_{ISC} = k_f + k_{IC}^0 \exp\left(\frac{-E_{IC}}{RT}\right) + k_{ISC}^0 \exp\left(\frac{-E_{ISC}}{RT}\right) + k_{ISC}(0) \quad (2)$$

Solvent Polarity Influence on Internal Conversion. The IC rate constant k_{IC} of 1N5, 1DMAN, and 1N4 is much larger in *n*-hexane than in acetonitrile (Table 1). With 1N5, for example, k_{IC} equals 1.2×10^{10} s^{-1} in *n*-hexane against 1×10^8 s^{-1} in acetonitrile. For 1N4 and 1DMAN a similar result is obtained. These decreases in k_{IC} are caused mainly by the activation energy E_{IC}, which is considerably larger in acetonitrile than in *n*-hexane,[10] whereas the preexponential factor k_{IC}^0 even slightly increases, with an average value $\sim 1.3 \times 10^{13}$ s^{-1} in *n*-hexane and $\sim 3.5 \times 10^{13}$ s^{-1} in acetonitrile, see Table 1.

To explain the increase of E_{IC} with solvent polarity in the case of 1DMAN, an energy gap model has been introduced.[10] In the context of this model, invoking vibronic coupling between the two lowest excited singlet states S_1 and S_2, the observed decrease of the IC rate with increasing solvent polarity is explained by assuming an increase in $\Delta E(S_1,S_2)$ when the solvent polarity becomes larger. This is caused by a more strongly polar character of the S_1 as compared with the S_2 state.[10] It is thereby assumed that the magnitude of E_{IC} is directly related to that of $\Delta E(S_1,S_2)$.

Radiative Rate Constant as a Function of Temperature. The temperature dependence of the ratio of the radiative rate constant k_f and the square of the solvent refractive index n_D for 1N5, 1N4, 1DMAN, and 1AN in *n*-hexane and acetonitrile is plotted in Figure 5. The plot is presented in this way, as k_f depends on n ($k_f \sim n^2$)[26] and n becomes smaller at higher temperatures.[27,28] For 1N5 and 1DMAN in *n*-hexane (Figure 5a), k_f/n_D^2 is practically constant upon heating the solution, whereas with 1AN and 1N4 a clear increase of k_f/n_D^2 is observed. In acetonitrile, k_f/n_D^2 also increases with increasing temperature for all aminonaphthalenes discussed here. This could indicate that in the aminonaphthalenes the admixture of the zero-order naphthalene states ^1L_b and ^1L_a with several CT states[29] changes with temperature.

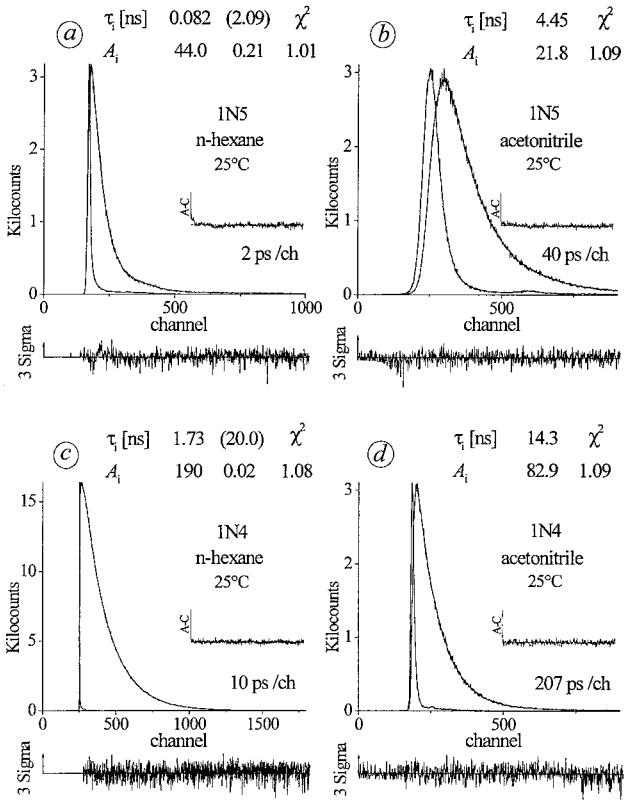

Figure 3. Fluorescence decays with decay times τ_i of 1N5 and 1N4 in *n*-hexane and acetonitrile at 25 °C. Excitation: (a) 299 nm, (b) 316 nm, (c) 300 nm, (d) 316 nm; emission: measured at the fluorescence maximum ~400 nm, see Figure 1. The τ_i values in parentheses are attributed to impurities. These are visible in *n*-hexane due to the small fluoresecence quantum yield of the 1-aminonaphthalenes in this solvent.

Molecular Structure of the 1-Aminonaphthalenes in S_0 and S_1. It was shown in the preceding sections that especially in the nonpolar solvent *n*-hexane an efficient internal conversion occurs with 1N5, 1DMAN, and 1N4 (in that order, see Table 1), with clearly larger rates than in the case of 1MAN and 1AN. Before an explanation for this photophysical behavior can be given, information on the molecular structure of these naphthylamines is presented. The difference in their molecular configuration in the ground and excited singlet state, in particular the twist angle θ between the amino group and the naphthalene plane (Figure 6), is discussed on the basis of absorption and fluorescence spectra, ^{1}H NMR chemical shifts, data on dipole moments, and ab initio calculations.

Ground-State Structure. Absorption Spectra. The absorption spectra of 1N4, 1N5, 1DMAN, 1MAN, and 1AN in *n*-hexane and acetonitrile at 25 °C are shown in Figure 1. In the spectrum of 1AN in *n*-hexane, the two overlapping S_1 and S_2 bands[30] are still visible, whereas these bands more strongly overlap for the other molecules. This indicates that the energy gap $\Delta E(S_1,S_2)$ decreases when the amino group is alkylated.[10] The energies of the maxima of these composite absorption bands are listed in Table 2. The absorption spectrum of 1MAN is red-shifted relative to that of 1AN, as is usual for *N*-methylated aromatic amines, such as for *N*-methylaniline as compared with aniline.[31] Contrary to what is found for *N*,*N*-dimethylaniline,[31] however, the red-shift upon introducing an additional methyl

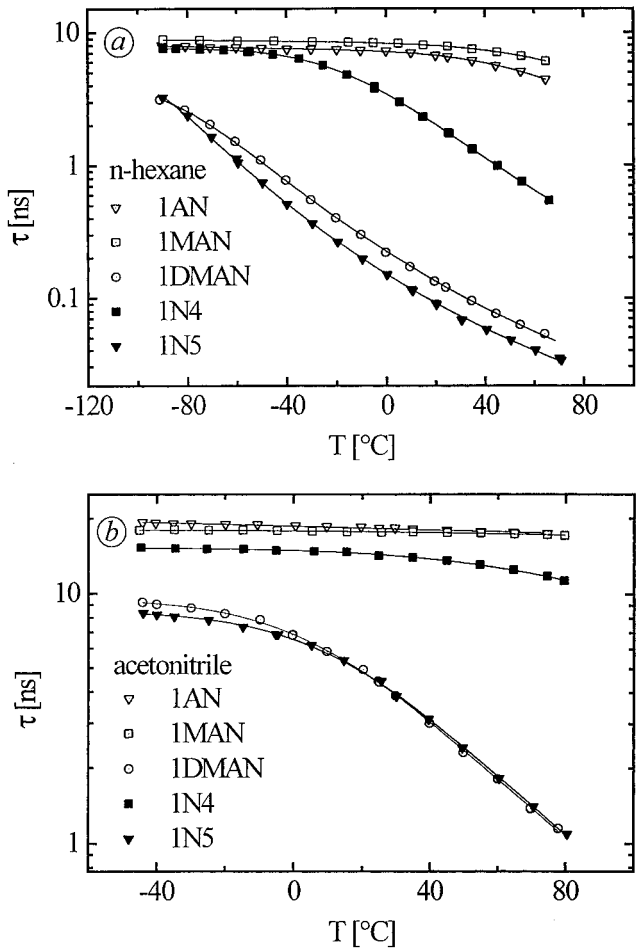

Figure 4. Fluorescence decay times τ of 1N5, 1N4, 1DMAN, 1MAN, and 1AN in (a) *n*-hexane and (b) acetonitrile as a function of temperature. The lines through the data points represent the fitting of the data with eq 2, giving the activation energies E_i and the preexponential factors k_i^0 (Table 1) of the internal conversion (IC) and intersystem crossing (ISC) processes in these 1-aminonaphthalenes.

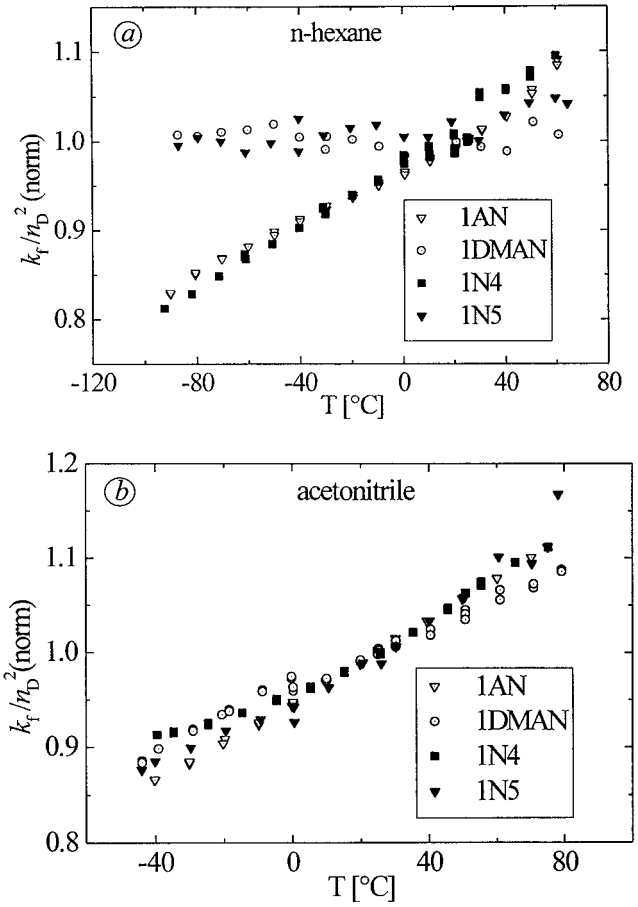

Figure 5. Plots of the ratio k_f/n_D^2 for 1N5, 1N4, 1DMAN, and 1AN in (a) *n*-hexane and (b) acetonitrile as a function of temperature. The radiative rate constant k_f is divided by the square of the refractive index n_D, see text and ref 28, and this ratio is normalized at 25 °C.

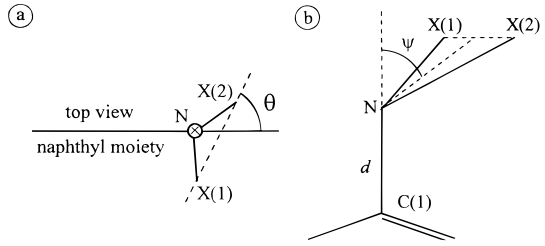

Figure 6. (a) Top view of a 1-aminonaphthalene used to define the amino twist angle θ between the amino group and the plane of the naphthyl moiety. (b) Partial side view of a 1-aminonaphthalene used to define the pyramidal angle ψ. N is the amino nitrogen, X(1) and X(2) are the amino substituents, and C(1) is the carbon atom in the 1-position of the naphthyl group.

group is not continued for 1DMAN: its absorption maximum is strongly blue-shifted with respect to that of 1AN and 1MAN. This blue-shift has been attributed to a larger twist angle ($\theta \sim 60°$) of the dimethylamino group in 1DMAN,[32−34] than that of the NH_2-substituent in 1AN, which is assumed to be only moderately twisted (θ between 20 and 30°) in the electronic ground state.[32−36] These data for θ have been derived from photoelectron spectra,[32,33] ground-state dipole moments,[34,35] and from a Hartree−Fock calculation coupled with high-resolution fluorescence excitation experiments in a supersonic jet.[36] The deviation from planarity of the naphthylamines in S_0 is due to the peri effect exerted by the hydrogen atom H8.[37]

In the case of the ring compounds 1N5 and 1N4, the absorption band in *n*-hexane and in acetonitrile (Table 2) is blue-shifted relative to 1MAN, although to a smaller extent than with 1DMAN. The blue-shift for 1N5 is larger than that for 1N4. This indicates that the amino group in 1N5 is more strongly twisted than in 1N4, with angles θ between those of 1DMAN and 1MAN or 1AN. This conclusion is supported by an analysis of ^{1}H NMR spectra, Stokes-shifts, and differences in the ground-state dipole moment μ_g as well as by ab initio calculations, to be discussed in the following sections.

The extinction coefficient ϵ^{max} of the lowest energy absorption maximum of 1DMAN in *n*-hexane (5100) is lower than that of 1MAN (7000), see Table 2 and Figure 1. This decrease is again attributed to the larger amino twist angle and the consequently increased amino/naphthyl decoupling in the case of 1DMAN. A similar phenomenon occurs in a series of anilines with blocking ortho substituents.[38,39] The observation (Table 2) that in *n*-hexane the ϵ^{max} values of 1N5 (6000) and 1N4 (6700) are between those of 1MAN and 1DMAN supports the conclusion that the amino twist angle of 1N5 is larger than that of 1N4, with values between those of 1DMAN and 1MAN. It should be noted that absorption spectra (spectral position and extinction coefficient) reflect the transition from the equilibrated S_0 ground state to the Franck−Condon (FC) excited states S_n and not to the relaxed S_1 state.

Structure of the Relaxed S_1 State. Fluorescence Spectra. Upon methylating the amino group of aromatic amines, their

TABLE 2: Maxima of the Absorption ($\tilde{\nu}_{abs}^{max}$) and Fluorescence ($\tilde{\nu}_{flu}^{max}$) Spectra, Stokes-Shift $\Delta\nu$(St), Energy of the First Excited Singlet State $E(S_1)$, and Extinction Coefficient ϵ^{max} of the Lowest Energy Absorption Maximum for Five 1-Aminonaphthalenes

	$\tilde{\nu}_{abs}^{max}$ [10^3 cm^{-1}]	$\tilde{\nu}_{flu}^{max}$ [10^3 cm^{-1}]	$\Delta\nu$(St) [10^3 cm^{-1}]	$E(S_1)$ [10^3 cm^{-1}]	ϵ^{max} [l mol^{-1} cm^{-1}]
			n-Hexane		
1N5	31.46	25.92	5.54	28.13	6000
1N4	30.66	25.56	5.10	27.98	6700
1DMAN	32.64	25.84	6.80	28.82	5100
1MAN	30.04	26.06	3.98	28.19	7000
1AN	31.44	26.52	4.92	28.96	5600
			Acetonitrile		
1N5	30.74	23.52	7.22	26.67	6200
1N4	30.38	23.16	7.22	26.40	
1DMAN	32.00	23.60	8.40	27.29	5300
1MAN	29.86	23.74	6.12	26.69	7100
1AN	30.74	23.88	6.86	27.28	5900

TABLE 3: ^{1}H NMR Chemical Shifts for the Proton H2 of Five 1-Aminonaphthalenes in $CDCl_3$

	δ(H2) [ppm]
1N5	6.98
1N4	6.56
1DMAN	7.09
1MAN	6.65
1AN	6.78

fluorescence spectra generally undergo a red-shift, due to an increase in the inductive effect of the substituent. Such a red-shift has been observed for the series aniline, *N*-methylaniline, and *N*,*N*-dimethylaniline,[40] as well as for the pair 2-amino-naphthalene and 2-(dimethylamino)naphthalene.[41,42] The fluorescence spectra in the group 1AN, 1MAN, and each of the three dialkylaminonaphthalenes 1DMAN, 1N5, and 1N4 in *n*-hexane and in acetonitrile at 25 °C (Figure 1 and Table 2) also show such a shift to the red. These observations indicate that the molecular structure of the equilibrated singlet excited state S_1 is similar for all five 1-aminonaphthalenes. As the amino twist angle θ in the relaxed S_1 state of 1AN is close to zero,[36] it is therefore concluded that the amino group of the other four 1-aminonaphthalenes likewise does not deviate appreciably from planarity.

Stokes-Shifts. This conclusion is supported by the data for the Stokes-shift $\Delta\nu$(St) between the maxima of the absorption and fluorescence spectra, which correlate with the twist angle θ in S_0 treated in the preceding sections. In *n*-hexane (Table 2), $\Delta\nu$(St) has the highest value for 1DMAN (6800 cm^{-1}) and then decreases in the same order as found for θ: 1N5 (5540 cm^{-1}), 1N4 (5100 cm^{-1}), 1AN (4920 cm^{-1}), and 1MAN (3980 cm^{-1}). In acetonitrile a similar correlation is found (Table 2). It hence follows that the differences in $\Delta\nu$(St) are determined by the ground-state amino twist angles.

^{1}H NMR Spectra. Differences in Amino Twist Angle. In the 1-aminonaphthalenes, the magnitude of the amino twist angle θ determines the electronic coupling between these groups, when the pyramidality of the amino nitrogen remains unchanged, see below. The extent of this coupling is determined by the twist-dependent delocalization of the lone-pair electrons of the amino nitrogen into the naphthalene nucleus: the mesomeric +M-effect.[39] The twist angle can then be monitored by measuring the chemical shifts δ in the NMR spectra,[12,43] see the data for δ(H2) in Table 3.

Upon the introduction of methyl groups in the amino substituents of an aromatic amine, it is to be expected that the chemical shift of the hydrogens next to the amino group progressively changes to lower ppm values, when the molecular structure such as the amino twist angle θ does not change. This is due to the inductive −I-effect,[39] based on the increase in the electron donor strength in the series NH_2, $NH(CH_3)$, $N(CH_3)_2$, which can be deduced from the amine oxidation potentials.[44] In accordance with this expectation, the δ(H2) of 1MAN (6.65 ppm) is shifted to smaller ppm values as compared with 1AN (6.78 ppm), see Table 3. In 1DMAN, however, a further upfield shift does not take place. Instead, a large downfield shift (to 7.09 ppm, Table 3) is observed, which is attributed to the substantial increase in the amino twist angle θ to ∼60°, as derived from the absorption spectra.

TABLE 4: Calculated and Experimental Ground-State (μ_g) and Excited-State (μ_e) Dipole Moments of Five 1-Aminonaphthalenes in Debye Units

	ρ^a [pm]	$\mu_g^{calcd_b}$ [D]	$\mu_g^{expt_c}$ [D]	$\Delta\mu^d$	μ_e [D]
1N5	420		(1.1)^e	7.0	8.1
1N4	410	1.45	(1.8)^f	6.2	8.0
1DMAN	410	0.84	1.05	6.1	7.1
1MAN	390	1.37	1.75	5.7	7.4
1AN	370	1.44	1.55	5.7	7.2

[a] Onsager radius, see eq 3. [b] From calculations (Gaussian 94, ref 51) using the HF−SCF method with a 6-31G* basis set. [c] Data from ref 35. [d] $\Delta\mu = \mu_c - \mu_g^{expt}$. [e] Experimental value assumed to be the same as for 1DMAN. [f] Calculated dipole moment for 1N4, scaled by the factor 1.25 for the ratio $\mu_g^{expt}/\mu_g^{calcd}$ of the tertiary amine 1DMAN.

For 1N5 with a δ(H2) value of 6.98 ppm, not much smaller than that of 1DMAN, a relatively large twist angle (close to 60°) is deduced. As the δ(H2) shift of 1N4 (6.56 ppm) is clearly smaller than that of 1N5 (Table 3), it is concluded that the azetidinyl group in 1N4 is less strongly twisted in the electronic ground state than the amino group in 1N5. Similar conclusions on the amino twist angles are reached in the previous sections.

Dipole Moments μ_g and μ_e. Solvatochromic Data. *Dipole Moment S_0.* The ground-state dipole moments μ_g of 1AN, 1MAN, and 1DMAN are listed in Table 4.[34,35] The dipole moment of 1MAN (1.75 D) is larger than that of 1AN (1.55 D), similar to what is observed upon alkylating the amino group in aniline[45] and 2-aminonaphthalene.[46] This increase is not continued, however, when a second methyl group is introduced in 1MAN: the dipole moment μ_g of 1DMAN (1.05 D) is considerably smaller than that of 1MAN and 1AN. The decrease in μ_g for 1DMAN has been attributed to the twist of the dimethylamino group, causing an electronic decoupling between this group and the naphthyl moiety,[34,35] as discussed above. For 1N4 and 1N5, experimental μ_g data are not available, therefore calculated values are employed (Table 4).

Dipole Moment S_1. The dipole moment μ_e of the molecules in the equilibrated S_1 excited state listed in Table 4 are derived from solvatochromic measurements. In a plot of the fluorescence band maxima (see Figure 1 and Table 1) against the solvent polarity parameter $f - f'$ the slope is equal to $\mu_e(\mu_e - \mu_g)/\rho^3$, see eqs 3 and 4.[48,49] The value taken for the equivalent spherical radius ρ of the solute molecule obviously is of great importance in the evaluation of these data. A number of methods for the determination of ρ are available.[50] The μ_e data in Table 4 are based on an Onsager radius ρ calculated by using the assumption that the molecular density equals unity. It is seen that the dipole moment of the 1-aminonaphthalenes increases substantially upon excitation, from ∼1.5 D for μ_g, to values between 7 and 8 D for μ_e in the equilibrated S_1 state (Table 4).

$$\tilde{\nu}_{flu} = \frac{-1}{4\pi\epsilon_0}\frac{2}{hc\rho^3}\mu_e(\mu_e - \mu_g)(f - f') + \text{constant} \qquad (3)$$

On the basis of these data, it is concluded that the electronic

$$f - f' = \frac{(\epsilon - 1)}{(2\epsilon + 1)} - \frac{(n^2 - 1)}{(2n^2 + 1)} \qquad (4)$$

properties and hence the molecular structure of 1DMAN, 1N4, and 1N5 in the relaxed S_1 state are similar to those of 1AN and 1MAN. The amino group of the last two molecules is considered to be practically planar in S_1, as discussed above. This means that especially for 1DMAN and 1N5, strongly twisted in S_0, and to a smaller extent also for 1N4, 1MAN, and 1AN, a large change in amino twist angle θ takes place upon reaching the equilibrated S_1 state. The same conclusion was reached from the large Stokes-shift $\Delta\nu$(St) of the two former molecules (Table 2).

Ab Initio Hartree−Fock Calculations. Ab initio Hartree−Fock (HF) calculations (Gaussian 94,[51] 6-31G* basis set) were performed on the 1-aminonaphthalenes in the electronic ground state. The results of these HF−SCF calculations are listed in Table 5. The amino twist angle θ has the largest value (60°) for 1DMAN, in good agreement with the experimental results discussed previously. For 1N4 an intermediate θ value (36°) is obtained, larger than that of 1MAN (15°) and 1AN (22°).

The pyramidality of the amino nitrogen does not differ strongly for the 1-aminonaphthalenes, with angles ψ between 38° for 1MAN and 47° for 1AN. For 1DMAN, 1N4, and 1MAN, having similar pyramidal angles ψ, the length d of the N−C(1) bond (Figure 6) is correlated with the twist angle θ, showing that the electronic decoupling of the amino and naphthyl moieties increases with θ.

Summary on Amino Twist Angles in S_0 and S_1. On the basis of the calculations and experimental data presented here for the 1-aminonaphthalenes, it is concluded that their amino twist angle depends on the structure of this group. The dimethylamino group in 1DMAN ($\theta \sim 60°$) and the pyrrolidinyl substituent in 1N5 are strongly twisted out of the naphthalene plane. For 1N4 an intermediate value for the twist angle is obtained, whereas the angle θ is considerably smaller for 1MAN and 1AN (~20°).

In the equilibrated S_1 state, in contrast, the naphthylamines have a similar molecular structure with a planar amino group, as deduced from their fluorescence spectra (Stokes-shifts) and radiative rate constants. The structural similarity of the S_1 state together with the different amino twist angle in the ground state S_0, is reflected in the differences in Stokes-shift (see Table 2).

Mechanism of Internal Conversion. Influence of Vibronic Coupling and Amino Twist Angle. The occurrence of efficient IC in 1DMAN and the other 1-aminonaphthalenes discussed here, is attributed to vibronic coupling between the two lowest excited singlet states S_1 and S_2 caused by the small energy gap $\Delta E(S_1,S_2)$.[10] The mechanistic importance of the ground-state amino twist angle θ can be deduced from the fact that a linear correlation exists between log k_{IC} and θ, see Figure 7 (Tables 1 and 5). In accordance with this correlation, only a weak IC process ($k_{IC} \sim 1 \times 10^7$ s^{-1}) takes place in the case of 1MAN and 1AN, for which molecules relatively small amino twist angles are calculated.

For the IC process occurring in the present 1-aminonaphthalenes, with an amino twist angle between 60° and 15° in S_0, the following mechanism is adopted, see Figure 8. After excitation to a still twisted S_1(FC) state, a fast equilibration process of the amino group structure sets in, toward a smaller twist angle. From the planar equilibrated S_1 state, a thermally activated IC reaction to S_0 then starts. When the energy gap $\Delta E(S_1,S_2)$ is sufficiently small, the S_1 potential energy surface is flattened by vibronic coupling between S_1 and S_2.[52,53] This leads to an increase of the isoenergetic vibrational overlap between the S_1 and S_0 surfaces (Figure 7), which overlap is further enhanced by the horizontal shift ($\Delta\xi$) of these potential energy surfaces, depending on the difference in amino twist angle. The height of the IC activation energy E_{IC} depends on the strength of the vibronic coupling, related to $\Delta E(S_1,S_2)$, and the shift $\Delta\xi$

TABLE 5: Results from ab Initio Calculations, Gaussian 94 (ref 51), HF−SCF Method with a 6-31G* Basis Set (See Figure 6)

	1N4	1DMAN	1MAN	1AN
θ [°][a]	36	60	15	22
d [pm][b]	140.5	142.4	139.7	140.4
Σ(N) [°][c]	337	342	344	335
ψ [°][d]	38	41	38	47

[a] Amino twist angle. [b] N−C(1) bond length. [c] Sum of the valence angles between the amino nitrogen and its neighboring carbon atoms. [d] Pyramidal angle.

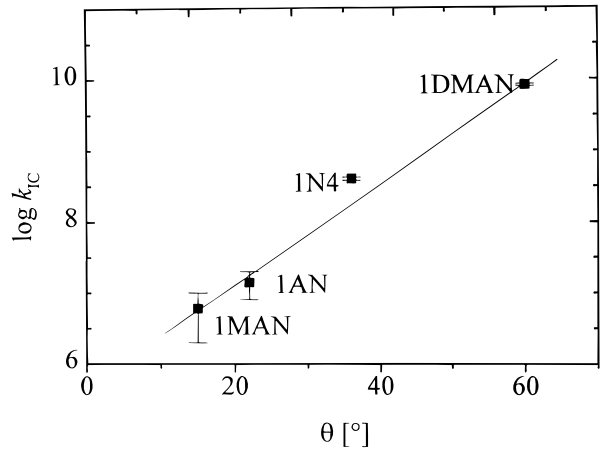

Figure 7. Plot of the logarithm of the internal conversion rate constant k_{IC} (in *n*-hexane at 25 °C) against the amino twist angle θ of 1AN, 1MAN, 1N4, and 1DMAN.

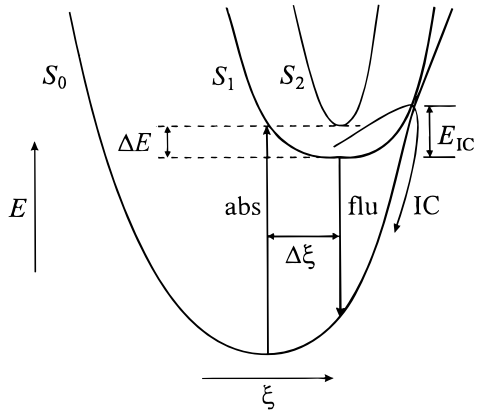

Figure 8. Potential surfaces of the electronic ground state S_0 and the two lowest excited singlet states S_1 and S_2 for the 1-aminonaphthalenes undergoing internal conversion (IC). The reaction coordinate ξ involves the amino twist angle. Light is absorbed to a Franck−Condon S_1 state, and fluorescence occurs after relaxation. The surface of S_1 is flattened by vibronic coupling with S_2. E_{IC} is the activation energy for the nonadiabatic IC reaction from the equilibrated S_1 state to S_0. $\Delta E(S_1,S_2)$ is the energy gap between S_1 and S_2.

governed by the amino twist angle. The energy gap $\Delta E(S_1,S_2)$ becomes larger with increasing solvent polarity,[10] which is responsible for the larger E_{IC} barriers and hence smaller IC rate constants in acetonitrile as compared with *n*-hexane.

Comparison of IC in Aminonaphthalenes with CT in Aminobenzonitriles. The IC process in 1N4 is clearly slower than in 1N5 and 1DMAN, caused by an increase in the IC activation energy E_{IC}. A similar phenomenon has been observed for the CT reaction of 4-aminobenzonitriles upon replacing the dimethylamino group in DMABN by an azetidinyl (P4C) or a pyrrolidinyl (P5C) substituent,[1−5] as mentioned in the Introduction. The reasons for the decrease in reaction efficiency are different, however. In the present case of the 1-aminonaphthalenes, the relatively large value for E_{IC} of 1N4 is attributed to the smaller amino twist angle θ of 1N4 as compared with 1N5 and 1DMAN, whereas with P4C the increase in the CT activation energy E_{CT} relative to that for P5C and DMABN has been explained by a larger barrier for the latter compounds of the configurational change of the amino group from pyramidal to planar.[1−5]

Conclusion

With 1N5 and 1DMAN, and to a smaller extent also with 1N4, a fast thermally activated internal conversion reaction takes place in *n*-hexane. This process becomes much slower in the polar solvent acetonitrile, caused by a polarity-dependent increase in the IC activation energy E_{IC}. An increase in E_{IC} also leads to a less efficient internal conversion with 1MAN and 1AN than with the three other naphthylamines.

A correlation is found between the efficiency of the IC process in the 1-aminonaphthalenes and the structure of their amino group in the electronic ground state, in particular the twist angle θ of this group relative to the naphthalene plane. For 1N5 and 1DMAN, with an amino twist angle of ∼60°, the IC rate is considerably larger than for the moderately twisted 1N4. With 1MAN and 1AN, having a relatively small θ value (∼20°), the IC efficiency is strongly reduced as compared with 1N5, 1DMAN, and 1N4.

In the equilibrated S_1 state, in contrast to S_0, the 1-aminonaphthalenes all have a planar structure, as deduced from the similarity of their fluorescence spectra and radiative rate constants. The IC reaction is governed by an increase in the interaction between the potential energy surfaces of S_1 and S_0, due to the following two effects. In the first place, the vibronic coupling between S_1 and S_2, which is promoted by a small energy gap $\Delta E(S_1,S_2)$. This coupling flattens the S_1 potential energy surface and leads to an increased isoenergetic vibrational overlap between S_1 and S_0. The coupling between the S_1 and S_0 surfaces is further enlarged by bringing them closer together as a consequence of the horizontal shift caused by the difference in the amino twist angle. The increase in E_{IC} when the solvent polarity becomes larger, is attributed to a preferential stabilization of the S_1 state relative to S_2, due to the more polar character of the former state. This stabilization results in a larger energy gap between S_1 and S_2, which leads to a decrease in the vibronic coupling between these two states.

Acknowledgment. We thank Dr. S. Tobita and Mr. K. Suzuki, Gunma University, for communicating their results on the fast internal conversion process in 1N5 prior to publication.

References and Notes

(1) Zachariasse, K. A.; von der Haar, Th.; Leinhos, U.; Kühnle, W. *J. Inf. Rec. Mats.* **1994**, *21*, 501.

(2) von der Haar, Th.; Hebecker, A.; Il'ichev, Yu. V.; Jiang, Y.-B.; Kühnle, W.; Zachariasse, K. A. *Rec. Trav. Chim. Pays-Bas* **1995**, *114*, 430.

(3) von der Haar, Th.; Hebecker, A.; Il'ichev, Yu. V.; Kühnle, W.; Zachariasse, K. A. In *Fast Elementary Processes in Chemical and Biological Systems*, Lille, France, 1995, *AIP Conf. Proc.* **1996**, *364*, 295.

(4) Zachariasse, K. A.; Grobys, M.; von der Haar, Th.; Hebecker, A.; Il'ichev, Yu. V.; Kühnle, W.; Morawski, O. *J. Inf. Recording* **1996**, *22*, 553.

(5) Zachariasse, K. A.; Grobys, M.; von der Haar, Th.; Hebecker, A.; Il'ichev, Yu. V.; Jiang, Y.-B.; Morawski, O.; Kühnle, W. *J. Photochem. Photobiol. A: Chem.* **1996**, *102*, 59.

(6) Rückert, I.; Zachariasse, K. A. Unpublished results.

(7) Ayuk, A. A.; Rettig, W.; Lippert, E. *Ber. Bunsen-Ges. Phys. Chem.* **1981**, *85*, 553.

(8) Druzhinin, S. I.; Uzhinov, B. M. *Theor. Exp. Chemistry* **1982**, *18*, 565.

(9) Meech, S. R.; O'Connor, D. V.; Phillips, D.; Lee, A. G. *J. Chem. Soc., Faraday Trans. 2* **1983**, *79*, 1563.

(10) Zachariasse, K. A.; Grobys, M.; von der Haar, Th.; Hebecker, A.; Il'ichev, Yu. V.; Morawski, O.; Rückert, I.; Kühnle, W. *J. Photochem. Photobiol. A: Chem.* **1997**, *105*, 373.

(11) Suzuki, K.; Tanabe, H.; Tobita, S.; Shizuka, H. *J. Phys. Chem. A* **1997**, *101*, 4496.

(12) Ernst, L. *Z. Naturforsch.* **1975**, *30B*, 794.

(13) Suhr, H.; Grube, H. *Ber. Bunsen-Ges. Phys. Chem.* **1966**, *70*, 544.

(14) Deady, L. W.; Topsom, R. D.; Hutchinson, R. E. J.; Vaughan, J.; Wright, G. J. *Tetrahedron Lett.* **1968,** 1773.

(15) Lohmann, J. *Chem. Ber.* **1891**, *24*, 2631.

(16) Tobias, G. *Chem. Ber.* **1882**, *15*, 2443.

(17) Zachariasse, K. A.; Duveneck, G.; Busse, R. *J. Am. Chem. Soc.* **1984**, *106*, 1045.

(18) Leinhos, U.; Kühnle, W.; Zachariasse, K. A. *J. Phys. Chem.* **1991**, *95*, 2013.

(19) Carmichael, I.; Helman, W. P.; Hug, G. L. *J. Phys. Chem. Ref. Data* **1987**, *16*, 239.

(20) Wintgens, V.; Valat, P.; Kossanyi, J.; Demeter, A.; Biczok, L.; Berces, T. *New J. Chem.* **1996**, *20*, 1149.

(21) Nemes, P.; Demeter, A.; Biczok, L.; Berces, T.; Wintgens, V.; Valat, P.; Kossanyi, J. *J. Photochem. Photobiol. A: Chem.* **1998**, *113*, 225.

(22) Carmichael, I.; Hug, G. L. *J. Phys. Chem. Ref. Data* **1986**, *15*, 1.

(23) Lamola, A. A.; Hammond, G. S. *J. Chem. Phys.* **1965**, *43*, 2129.

(24) Suzuki, S.; Fujii, T.; Imal, A.; Akahori, H. *J. Phys. Chem.* **1977**, *81*, 1592.

(25) An activation energy of intersystem crossing $\Phi_{ISC} = 5$ kJ/mol was obtained from the analysis of the decay times τ of 1DMAN in isopentane in the low-temperature region (ref 6).

(26) Timmermans, J. *Physico-Chemical Constants of Pure Organic Compounds*, Vol. I.; Elsevier: New York, 1950.

(27) Birks, J. B. *Photophysics of Aromatic Molecules*; Wiley: London, 1970.

(28) The data for n_D at the various temperatures were calculated from the corresponding solvent densities ρ by using the Lorentz−Lorenz equation $\rho \sim (n^2 - 1)/(n^2 + 2)$. The values for ρ and n_D (25 °C) were taken from the following references: (a) Landolt-Börnstein; *Numerical Data and Functional Relationships in Science and Technology*, New Series, Vol. III/38b; Martienssen, W., Ed.; Springer: Berlin, 1996. (b) Rossini, F. D.; Pitzer, K. S.; Arnett, R. L.; Braun, R. M.; Pimentel, G. C. *Selected Values of Physical and Thermodynamic Properties of Hydrocarbons and Related Compounds*; Carnegie Press: Pittsburgh, PA, 1953. (c) Timmermans, J. *Physico-Chemical Constants of Pure Organic Liquids*, Vol. I.; Elsevier: New York, 1950.

(29) Suzuki, S.; Fujii, T.; Baba, H. *J. Mol. Spectrosc.* **1973**, *47*, 243.

(30) Whipple, M. R.; Vasak, M.; Michl, J. *J. Am. Chem. Soc.* **1978**, *100*, 6844.

(31) Jaffé, H. H.; Orchin, M. *Theory and Applications of Ultraviolet Spectra*; Wiley: New York, 1964; p 410.

(32) Maier, J. P. *Helv. Chim. Acta* **1974**, *57*, 994.

(33) Utsunomiya, C.; Kobayashi, T.; Nagakura, S. *Bull. Chem. Soc. Jpn.* **1975**, *48*, 1852.

(34) Lumbroso, H.; Berlot, J.; Bertin, D. M.; Renault, J. *C. R. Acad. Sci. Paris C* **1970**, *270*, 1204.

(35) Le Fèvre, R. J. W.; Sundaram, A. *J. Chem. Soc.* **1962**, 4756.

(36) Berden, G.; Meerts, W. L.; Plusquelic, D. F.; Fujita, I.; Pratt, D. W. *J. Chem. Phys.* **1996**, *104*, 3935.

(37) Balasubramaniyan, V. *Chem. Rev.* **1966**, *66*, 567.

(38) Wepster, B. M. *Rec. Trav. Chim. Pays-Bas* **1958**, *77*, 491.

(39) Murrell, J. N. *The Theory of the Electronic Spectra of Organic Molecules;* Methuen: London, 1963; Chapter 11.

(40) Köhler, G. *J. Photochem.* **1987**, *38*, 217.

(41) Lentz, P.; Blume, H.; Schulte-Frohlinde, D. *Ber. Bunsen-Ges. Phys. Chem.* **1970**, *74*, 484.

(42) Seliskar, C. J.; Brand, L. *J. Am. Chem. Soc.* **1971**, *93*, 5405.

(43) Zweig, A.; Lancaster, J. E.; Neglia, M. T. *Tetrahedron* **1967**, *23*, 2577.
(44) *Encyclopedia of Electrochemistry of the Elements*, Vol. XV.; Bard, A. J., Ed.; Dekker: New York, 1984.
(45) Few, A. V.; Smith, J. W. *J. Chem. Soc.* **1949**, 3057.
(46) Baliah, V.; Balasubramaniyan, V. *J. Indian Chem. Soc.* **1993**, *70*, 755.
(47) Schreiner, P.; Zachariasse, K. A. In preparation.
(48) Lippert, E. *Z. Elektrochem.* **1957**, *61*, 962.
(49) Liptay, W. In *Excited States*, Vol. 1; Lim, E. C., Ed.; Academic Press: New York, 1974; p 129.
(50) Il'ichev, Yu. V.; Kühnle, W.; Zachariasse, K. A. *Chem. Phys.* **1996**, *211*, 441.
(51) Frisch, M. J.; Trucks, G. W.; Schlegel, H. B.; Gill, P. M. W.; Johnson, B. G.; Robb, M. A.; Cheeseman, J. R.; Keith, T.; Petersson, G. A.; Montgomery, J. A.; Raghavachari, K.; Al-Laham, M. A.; Zakrzewski, V. G.; Ortiz, J. V.; Foresman, J. B.; Cioslowski, J.; Stefanov, B. B.; Nanayakkara, A.; Challacombe, M.; Peng, C. Y.; Ayala, P. Y.; Chen, W.; Wong, M. W.; Andres, J. L.; Replogle, E. S.; Gomperts, R.; Martin, R. L.; Fox, D. J.; Binkley, J. S.; Defrees, D. J.; Baker, J.; Stewart, J. P.; Head-Gordon, M.; Gonzalez, C.; Pople, J. A. *Gaussian 94*, Revision B.2; Gaussian, Inc.: Pittsburgh, PA, 1995.
(52) Hochstrasser, R. M.; Marzzacco, C. A. In *Molecular Luminescence;* Lim, E. C., Ed.; Benjamin: New York, 1969; p 631.
(53) (a) Lim, E. C.; Huang, C.-S. *J. Chem. Phys.* **1974**, *61*, 736. (b) Fischer, G. *Vibronic Coupling*; Academic: London, 1984.